ATMOSPHERIC STRUCTURE AT 130–200 KM ALTITUDE FROM OBSERVATIONS ON GRENADE GLOW CLOUDS DURING 1962–63

By K. H. LLOYD* and L. M. SHEPPARD*

[*Manuscript received November* 8, 1965]

Summary

Glows have been observed at night and at twilight following detonation of aluminized grenades in the altitude range 100–200 km. From observations made with equipment located on the ground, the variation with time of the radiance distribution across the glow clouds has been determined, and this is used to calculate the molecular diffusion coefficient in the region 130–200 km. The derivation of atmospheric density and temperature from the molecular diffusion coefficient is discussed in some detail, and results are presented for a number of Skylark rocket firings at Woomera during 1962 and 1963. The estimated maximum error in density is 30% and in temperature 15%. Within the limit of these errors, no diurnal effects have been detected. Above 150 km altitude, the observations have shown that the initial cloud radii are two to three times greater than predicted. A qualitative explanation of this effect is given by combining blast-wave theory with molecular-flow theory.

I. INTRODUCTION

Aluminized grenades exploded in the upper atmosphere in the altitude range 100–200 km produce a glowing cloud whose size increases with time. At night, the glow results from chemiluminescent reactions occurring between the products of the grenade explosion and the ambient atmosphere; for a sunlit cloud at twilight, the light emitted from the cloud is a result of resonant scattering of the Sun's rays by molecules of aluminium oxide. When the expansion of the glow cloud is due to molecular diffusion, observations on the rate of expansion give the molecular diffusion coefficient. In a previous paper, Johnson and Lloyd (1963) presented some results for the molecular diffusion coefficient, together with a description of the scanning photometer used to obtain the results. For all later trials, observations have been made with cameras as well as with the scanning photometer. The present paper gives final results for all glow clouds that were observed during 1962 and 1963, and gives a brief description of the method that has been used to analyse the photographic records. Preliminary results for 1962 have been published previously (Sheppard and Lloyd 1964).

Using the relation between density and molecular diffusion coefficient given by the kinetic theory of gases, the upper atmospheric density may be derived from the observed diffusion coefficient. The relation involves molecular weight, collision diameter, and temperature. The first two can be estimated with sufficient accuracy from model atmospheres and laboratory experiments; however, the upper atmospheric temperature is very variable, and an estimate of this is derived from the rate of change of observed diffusion coefficient with altitude.

* Weapons Research Establishment, Salisbury, S. Aust.

The upper atmospheric winds determined from the drift of the glow clouds have been published by Groves (1963*a*) as part of the Skylark research program.

Reviews of atmospheric measurements in the altitude range 100–200 km have been given by Whitehead (1963) and by Champion (1965). Whitehead examined density measurements in the *E* region of the ionosphere, near 120 km altitude, while Champion assessed some recent measurements of atmospheric structure. These reviews emphasize that there is a need to make measurements of the atmosphere in the altitude region 100–200 km. The present paper shows how the grenade glow cloud technique can be used to provide additional atmospheric structure information for this important region of the upper atmosphere.

II. Equipment and Observations

All the grenade glow clouds were produced by the explosion of standard 1 lb grenades, except for two 25 g grenades that were exploded simultaneously on Skylark vehicle SL167 as a scale experiment. The standard 1 lb grenade carries 437 g of pyrotechnics containing about 40% aluminium by weight; reactions involving oxides of this element are believed to be responsible for the glow. Armstrong (1963) and Johnson (1965) have shown that sunlit glow clouds result primarily from scattering of the incident Sun's rays by AlO molecules. The reactions that give rise to night-time glow clouds are not known, but it is suspected that they involve the reaction of an aluminium oxide with atomic oxygen in the atmosphere to give Al_2O_3. Therefore, any theoretical values for the glow cloud behaviour will be calculated by assuming that it consists initially of 437 g of atoms and molecules and that the significant reactive contaminant is AlO.

Results were obtained from the scanning photometer, which has been described by Johnson and Lloyd (1963), from the Baker–Nunn camera, and from two Shackman cameras. Examples of radiance results are given in Figure 1. Before discussion of the observations, a brief description will be given of the photographic method.

The Baker–Nunn camera has a 20 in. focal length and an aperture of $f/1$. It uses a Royal X Pan 70 mm film. The field of view is 5° by 25°, and the shutter opens for 20% of the framing time which is any multiple of 2 sec. The Shackman camera has an 85 mm focal length and an aperture of $f/1{\cdot}5$. It is shutterless and has a fast film wind. The exposure time for each frame is normally chosen to lie somewhere between 2 and 20 sec.

The image of the glow cloud on the photographic negative is analysed using a scanning microdensitometer, which has a small spot of light scanning slowly to and fro across the image of the glow. The transmitted light falls on a photomultiplier connected to a logarithmic amplifier whose output is fed into an X-Y recorder, which, therefore, traces out the density cross section of the glow. For each glow cloud, two scans are made at right angles to one another in order to verify that the cloud is spherically symmetric. Knowing the exposure–density calibration for the film, the variation in radiance across the glow cloud can then be found, and thus the effective radius r_e can be determined at any time.

Figure 2 presents plots of r_e^2 against time for a glow cloud in the molecular diffusion region. It is seen that there is good agreement between the results from the Shackman cameras, the Baker–Nunn camera, and the scanning photometer, thus confirming that there is little or no systematic error in the results. The definition of effective radius as the radius at which the cloud radiance has dropped to 1/e of its peak value applies only to clouds that have a Gaussian radiance distribution (see Fig. 1(*a*)). For glow clouds that show a non-Gaussian behaviour, as illustrated in

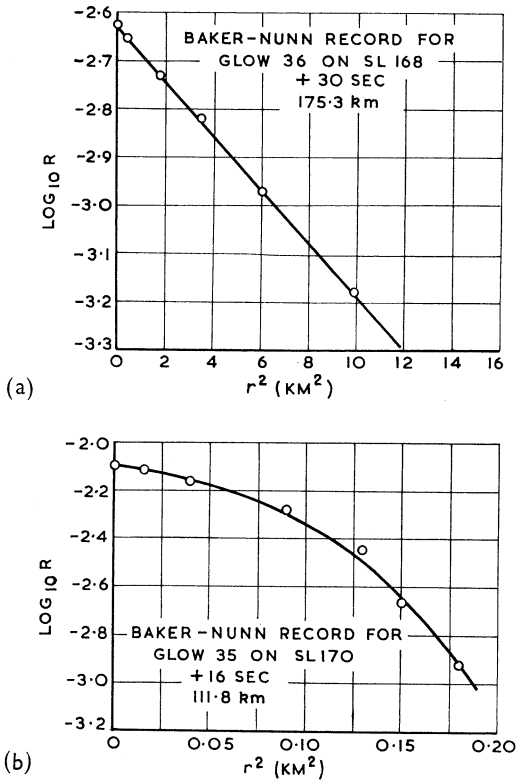

Fig. 1.—Radiance variation across glow cloud. (*a*) Typical Gaussian cloud; (*b*) typical non-Gaussian cloud.

Figure 1(*b*), the effective radius is calculated from the slope of the straight segment of the plot of $\log_{10} R$ against r^2, even though the analysis of the glow cloud in terms of a Gaussian model is not strictly valid. However, provided that the non-Gaussian part of the cross section is relatively insignificant, the results may be used, but with caution.

The commonest departure from a non-Gaussian shape is the convex form shown in Figure 1(*b*). Sometimes the curve is convex throughout, and sometimes there is a Gaussian portion at lower radiance levels. The non-Gaussian shape is more marked during the early development of the glow clouds, especially at the lower altitudes. Our observations are summarized in Figure 3, which gives the times

after which the radiance distribution is substantially Gaussian, as a function of altitude. There is apparently no difference between twilight and night-time glow clouds. Since there is no clear division between near-Gaussian and non-Gaussian

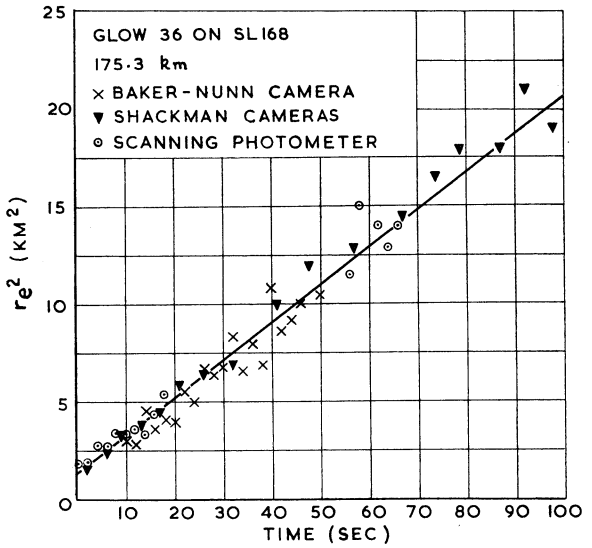

Fig. 2.—Example illustrating variation of r_e^2 with time.

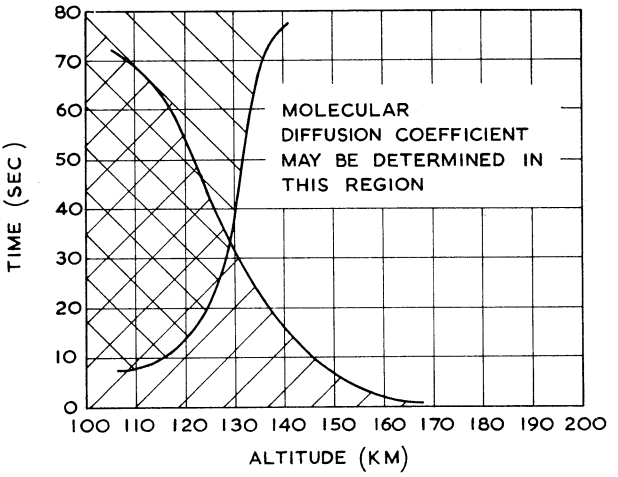

Fig. 3.—Regions in which diffusion coefficient may be determined using standard grenades. \\\\\ turbulent diffusion dominates expansion of glow cloud; ///// radiance distribution across glow cloud is markedly non-Gaussian.

profiles, the curve in Figure 3 is somewhat arbitrary; in the region below the curve, no effective radius may be satisfactorily measured, and in the vicinity of the curve the effective radius measurements should be examined carefully before they are used

to determine diffusion coefficients. A second boundary is given in Figure 3, showing the region where our observations indicate that turbulent diffusion dominates; in this region, r_e^2 does not vary linearly with time.

The results for all the glow clouds from the Skylark firings during October 1963 are given in Figure 4, which shows the square of the effective radius for various times as a function of altitude. The number of the trial to which the glow refers is

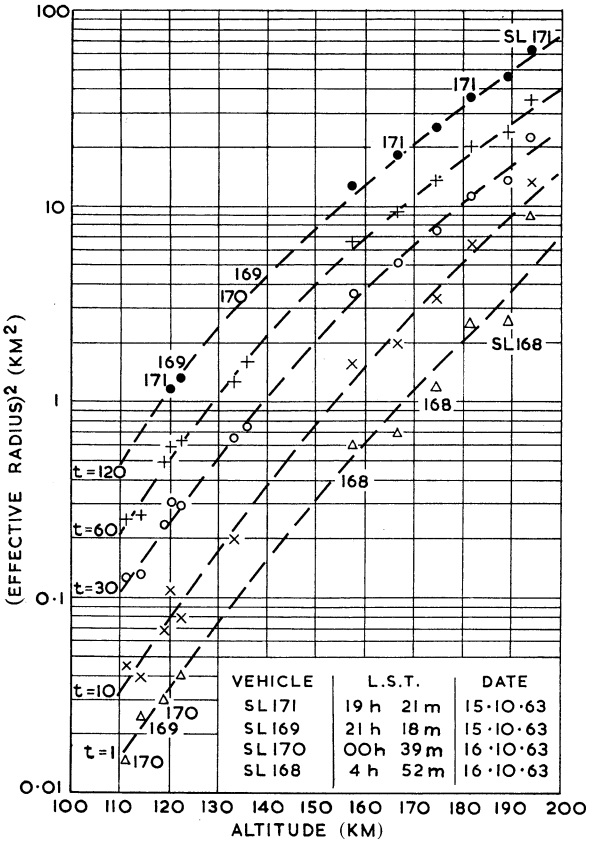

Fig. 4.—Variation of r_e^2 with altitude and time. (Time after grenade explosion indicated on each curve.)

noted above each series of points. Although effective radius has little meaning below about 130 km altitude, and certainly cannot be used for determining molecular diffusion coefficients, its values in this region are also plotted here. The scatter in Figure 4 is much greater at small times. This is because the proportional increase in effective radius with time is larger in the early stages of the expansion. Note that there is no evidence of a systematic trend of variation between the four firings; that is, within the accuracy of the results there is no diurnal effect. This is as would be expected from the observations of May (1963) and from the model atmospheres of Harris and Priester (1962), whose results indicate that the maximum diurnal change in density at 200 km altitude is about 20%.

III. Initial Cloud Radius

Figure 5 shows the initial radius calculated from the U.S. Standard Atmosphere 1962 (Champion, O'Sullivan, and Teweles 1962) on the assumption that the grenade forms 437 g of gas, that the peak contaminant density equals the ambient density ρ of the atmosphere, and that the density distribution is Gaussian. From these assumptions, it follows that the mass of gas m_E is equal to $\pi^{3/2}\rho r_0^3$; that is, the initial effective radius r_0 is $\pi^{-\frac{1}{2}}(m_E/\rho)^{\frac{1}{3}}$. The observed effective radius is much larger than the theoretical value at the higher altitudes, and the magnitude of this discrepancy increases rapidly with altitude. From the observed value of r_e^2, r_0 may be found and the initial

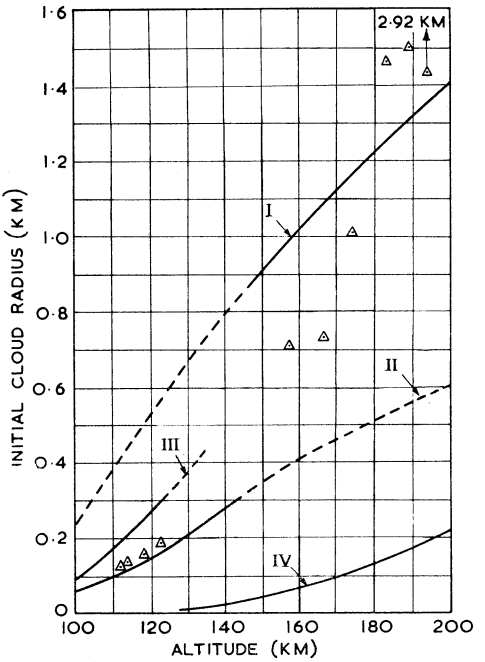

Fig. 5.—Initial cloud radius. Curve I: $r_0 = 0{\cdot}5(E_0/p)^{\frac{1}{3}}$, $E_0 = 2{\cdot}95\times10^6$ J; curve II: r_0(theory) $= \pi^{-\frac{1}{2}}(m_E/\rho)^{\frac{1}{3}}$, $m_E = 0{\cdot}437$ kg; curve III: m_E (Groves 1963*b*) $= 0{\cdot}437$ kg, $E_0 = 1{\cdot}44\times10^6$ J; curve IV: mean free path in atmosphere. Atmospheric data from U.S. Standard Atmosphere 1962. △ results from observations (see Fig. 4).

centre-point number density for the cloud may be calculated using $n_0 = N_0\pi^{-3/2}r_0^{-3}$, where N_0 is the number of contaminant molecules in the cloud; it seems that the initial peak number density is 10% and 0·4% of the ambient number density at 140 and 200 km altitude respectively. The reason for the large observed effective radius is not certain. If both the grenade explosion products and the shock-heated air were at a very high temperature, the diffusion coefficient would initially be much higher, and the cloud would expand very quickly at first. If this were so, the observed diffusion coefficient, given by the rate of increase of r_e^2, would be greater over the first few seconds; however, the observations show that this is not the case.

A grenade has a central core of tetryl which, on detonation, yields gaseous products at a temperature of about 4500°C and a pressure of about 200 000 atm having a flow speed of about 1500 m/sec behind the detonation wave. The aluminized mixture probably deflagrates, rather than detonates, because suboxides of aluminium are formed. This combustion requires a finite time and will not be complete before a rapid expansion of the central core of high pressure gas occurs. The fast moving AlO molecules formed are then retarded by collision with molecules of the ambient atmosphere. Chapman and Cowling (1952) have discussed the persistence of velocities (speed and direction) in molecular collisions. Use of their results shows that AlO molecules moving rapidly through an atmosphere consisting of molecules of half their molecular weight will lose, on average, about a third of their velocity at each collision. Because the AlO molecules are heavy, they will not be deflected very much in a collision, and so they will probably lose about a quarter of their speed at each collision. This means that, even if the initial speed of the AlO molecules is 1600 m/sec, corresponding to a temperature of 4500°C, their speed will be reduced to the ambient molecular speed (600–700 m/sec) after only three collisions with air molecules. When the cloud has expanded to ambient pressure, AlO molecules near the edge of the cloud will collide with as many air molecules as AlO molecules, so six collisions are then needed to slow down the fast moving AlO molecules. Six collisions correspond to travel through a distance radially outwards of about three mean free path lengths. Therefore, since the mean free path is insensitive to molecule speed, the initial cloud radius should be about three mean free path lengths greater than the theoretical prediction of Figure 5. The mean free path given by the U.S. Standard Atmosphere 1962 is plotted in Figure 5 and shows that, above 150 km altitude, the observed initial effective radius is approximately 10 times the mean free path and is more or less altitude-independent. Thus, this explanation is also unsatisfactory.

Alternatively, one might assume that all the AlO molecules will be at ambient temperature after mixing with three times their number of air molecules. When this occurs, some time after detonation of the grenade, the cloud radius will be 59% greater than the theoretical prediction of Figure 5. Hence, the initial effective radius might be 20–50% greater than the theoretical prediction. It seems that this explanation is also unsatisfactory, since the initial effective radii observed at 190 km altitude are about 200% greater than the theoretical predictions of Figure 5.

Another possible explanation can be deduced by combining simple blast-wave theory with free-molecule flow theory. According to Sedov (1959), there exists a central region of very low density for some considerable time after a point explosion. The low density region becomes larger as the ratio of specific heats γ decreases, and it probably trebles in size as γ decreases from $1\cdot4$ to $1\cdot2$. Denoting the energy released in the explosion by E_0, the ambient pressure by p, and the ambient density by ρ, an analysis of Sedov's results suggests that for $\gamma = 1\cdot2$, ρ_{centre} is less than $\frac{1}{3}\rho$ over the central region $r < (E_0/p)^{\frac{1}{3}}$ for times given by $0\cdot1 < (tE_0^{-\frac{1}{3}}\rho^{-\frac{1}{2}}p^{\frac{5}{6}}) < 10$; for the 1 lb grenade, $(E_0/p)^{\frac{1}{3}} \doteqdot 0\cdot4$–$3\cdot0$ km, and $E_0^{\frac{1}{3}}\rho^{\frac{1}{2}}p^{-\frac{5}{6}} \doteqdot 2$–$4$ sec over the altitude range 100–200 km. The gaseous products of the grenade explosion will expand to fill most of the central region, since this low density region exists for at least several seconds, and so the initial cloud radius is $r_0 \doteqdot 0\cdot5(E_0/p)^{\frac{1}{3}}$. The mean free path in the low density region

is about 10 times that in the local ambient atmosphere and is comparable with the initial cloud radius. This means that the initial expansion of the glow cloud can be virtually a free-molecule flow into the low density region, so that complete mixing with the air therein occurs. The rate of the free-molecule expansion is approximately equal to the mean molecular speed of the cloud molecules (Molmud 1960), i.e. about 1 km/sec. Therefore, it takes the cloud only about 1 sec to expand to its large initial effective radius. This is confirmed by the observations. Figure 5 shows comparisons between the observational results and the theoretical prediction, assuming that no mixing occurs, as well as the result given by $r_0 = 0{\cdot}5(E_0/p)^{\frac{1}{3}}$, which seems to represent the higher altitude results fairly well.

The initial cloud radius predicted by Groves (1963*b*), who used a simplified model to describe a similar grenade explosion, is also shown in Figure 5. It is interesting to note that the results of Groves (1963*b*) predict that there will be no shock wave formed above about 135 km altitude. We believe that shock waves will be formed at higher altitudes. At 160 km altitude, use of Sedov's (1959) simple results for point explosions indicates that the shock Mach number is 2 at a radius of about 0·7 km and, since the shock thickness is about four (atmospheric) mean free path lengths, there is just enough air available behind and near the shock wave for it to have been formed. No shock wave will be formed above about 180 km altitude.

A scale experiment was performed in April 1963, when two 25 g grenades were exploded simultaneously at 129 km altitude, and it was found that the initial effective radius was the same as for the standard 437 g grenade. This observation is consistent with the mean free path explanation given above, since a 50 g grenade at 129 km altitude is equivalent to a standard grenade at about 145 km altitude (Fig. 5); that is, the initial effective radius is nearly twice as large as the theoretical prediction for no mixing. However, even though there was no photographic evidence of merging glow clouds, the effective radius may have been a little larger than for a single 50 g grenade, because the two grenades could have exploded some distance (10–50 m) from one another. It is planned to carry out further scale experiments in the future to compare the behaviour of both large and small grenades at a number of different altitudes.

IV. Theory of Radiance of Glow Clouds

Theoretical models for the radiance of glow clouds have been given by Lloyd (1965). Only an outline of the analysis for the special case of optically thin glow clouds, with Gaussian particle densities, is given here. The governing differential equation is

$$\frac{\partial n}{\partial t} = D\left(\frac{\partial^2 n}{\partial r^2} + \frac{2}{r}\frac{\partial n}{\partial r}\right) - Kn, \tag{1}$$

with $$n(r, 0) = n_0 \exp(-r^2/r_0^2),$$

where D is the diffusion coefficient and Kn is a chemical reaction term (see, for example, Crank 1956). For either night-time or twilight glow clouds, it can be shown

that, at a distance r from the centre of the cloud, the surface radiance R is given by

$$R = \frac{R_0 \, e^{-Kt}}{(r_e/r_0)^2} \exp(-r^2/r_e^2), \tag{2}$$

where R_0 is the initial centre-point radiance, and $r_e^2 = r_0^2 + 4Dt$. From equation (2), it is clear that the radial distribution of radiance is best examined by plotting $\log R$ against r^2. An example of a Gaussian radiance distribution is given in Figure 1(*a*). Figure 1(*b*), on the other hand, shows a cloud to which the theoretical model cannot be applied.

If a sunlit twilight glow cloud is not very far above the Earth's shadow, the intensity of the sunlight incident on the glow is diminished by absorption and scattering in the lower layers of the Earth's atmosphere. Since the height of the Earth's shadow does not remain constant, the intensity of the sunlight falling on the cloud will change with time. If the time dependence of the incident solar flux in such cases is given by $F(t)$, equation (2) should be replaced by the more general expression

$$R = \frac{R_0 f(t)}{(r_e/r_0)^2} \exp(-r^2/r_e^2), \tag{3}$$

where $f(t) = F(t) \, e^{-Kt}$. The centre-point radiance at time t is given by

$$R_{\text{centre}} = R_0 (r_0/r_e)^2 f(t). \tag{4}$$

Experimental results on cloud radiance may be used to give two independent determinations of diffusion coefficient (Johnson and Lloyd 1963). The first, by Method A below, is based on the radial distribution of radiance, and the second, by Method B, is based on the centre-point radiance.

Method A.—From equation (3), it follows that

$$\frac{-0{\cdot}4343}{\partial(\log_{10} R)/\partial r^2} = r_e^2 = r_0^2 + 4Dt. \tag{5}$$

Thus, $\partial(\log_{10} R)/\partial r^2$ may be used to give the first estimates of D and r_0^2. This is the better method of calculating the diffusion coefficient.

Method B.—Integration of equation (3) gives, for the total radiant power (Lloyd 1965),

$$P = 4\pi^2 r_0^2 R_0 \, f(t), \tag{6}$$

that is,

$$P = 4\pi^2 r_e^2 R_{\text{centre}}; \tag{6a}$$

this enables the radiant power P to be calculated using the value of r_e^2 determined in Method A. The function $f(t)$ of equation (6) can now be calculated, and from equation (4) it follows that

$$1 + (4Dt/r_0^2) = f(t) \, (R_0/R_{\text{centre}}). \tag{7}$$

Equation (7) gives $4D/r_6^2$, from which a second estimate of the diffusion coefficient D may be made.

Provided that the glow has a Gaussian radiance distribution at all times, it follows that, if the early development of the cloud was not observed or if the initial data were not very accurate, the analysis described above could still be used; in these cases, time is measured from the time $t = t_1$ of the first reliable observation. For the results presented here, the initial values of centre-point radiance were rather inaccurate, and so equation (7) was used with a reference time of 10 sec; that is, $4D/r_6^2$ is determined at $t = 10$ sec. The results so obtained are compared with the corresponding results from Method A in order to confirm the validity of the theoretical diffusion model.

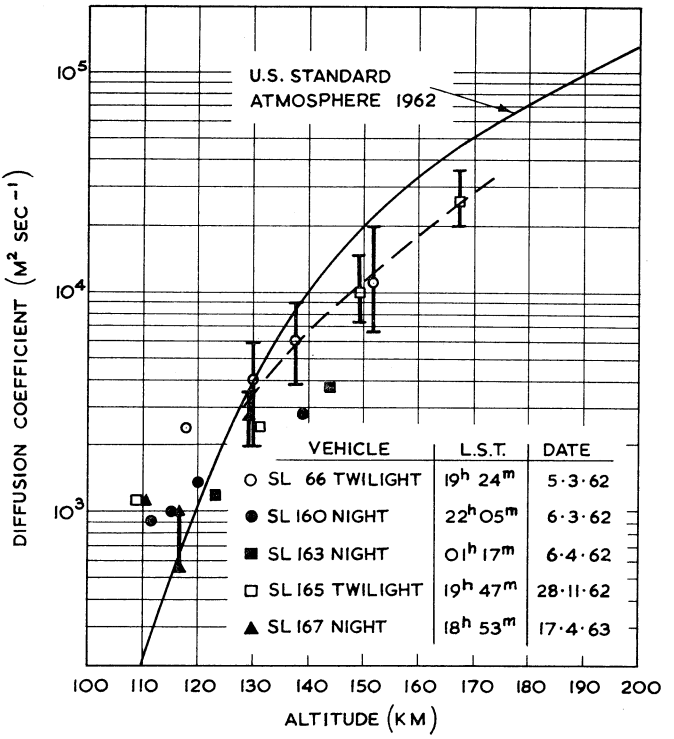

Fig. 6.—Diffusion coefficient from the earlier observations.

V. Observed Diffusion Coefficients

Figures 6 and 7 show the diffusion coefficient determined from the rate of change of r_6^2 with time (Method A) for the earlier and later set of firings respectively. Above 130 km altitude, the diffusion coefficient is a real molecular diffusion coefficient, and the results may be used to infer the atmospheric density. In the figures, some of the points carry bars indicating the maximum error, and, judging by the scatter in the diffusion coefficient results, the actual errors are less than the indicated maximum errors. There does not appear to be any diurnal effect.

Below 130 km altitude, turbulence becomes increasingly significant. Initially, r_e^2 increases linearly with time due to molecular diffusion, and, when the effective radius is comparable with the eddy size of the turbulence, turbulent diffusion dominates and there is a discontinuity in the plot of r_e^2 against time. For some results, it was possible to detect this discontinuity and so identify the time at which turbulent diffusion became predominant. In such cases, the slopes of the curve were measured before and after the discontinuity. The apparent diffusion coefficients given by these two slopes are both plotted in Figures 6 and 7 and the two values connected by a line. In all cases, the smaller diffusion coefficient refers to the molecular diffusion

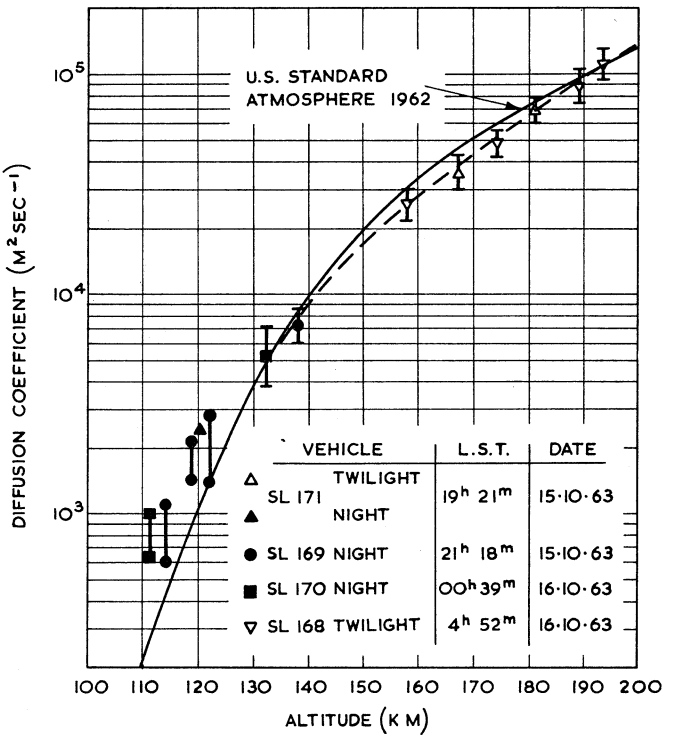

Fig. 7.—Diffusion coefficient from the October 1963 observations.

region. These molecular diffusion coefficients are less accurate than those for the higher altitudes, because of the small observation times, and so they have not been used to extend the results of Figures 6 and 7 to lower altitudes. Figure 3 shows, as a function of altitude, the times after which turbulence dominates the cloud expansion. It is clear that the non-Gaussian and turbulence effects between them prevent the molecular diffusion coefficient from being determined below about 130 km altitude.

Using the smoothed curves for r_e^2 from Figure 4, and those for D from Figure 7, the ratio $4D/r_e^2$ may be calculated for different times as a function of altitude. The curves are shown in Figure 8. It is immediately apparent that the ratio $4D/r_e^2$ is far more sensitive to changes in time than to changes in altitude. Comparisons of results for $4D/r_e^2$ derived from Methods A and B of Section IV are shown in the figure, with a

reference time of 10 sec after the grenade explosions. Good agreement is obtained. Figure 8 also gives results deduced from Method B assuming that the radiant power P is independent of time. Two results are very unsatisfactory; as a consequence, the variation of P with time must be incorporated in Method B. The results for Skylark SL168 are particularly interesting because the rising Sun caused $F(t)$, and hence P, to increase with time. It follows that, early on in the life of these two glow clouds, the intensity of the Sun's incident rays had been reduced substantially by absorption and scattering in the lower layers of the Earth's atmosphere.

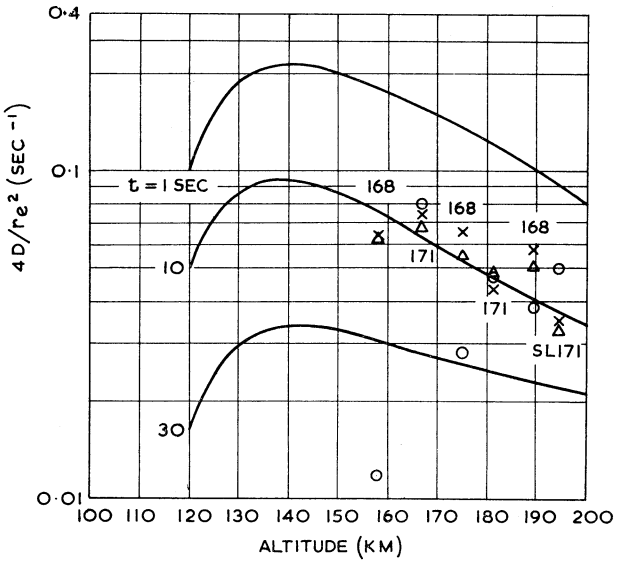

Fig. 8.—Altitude variation of $4D/r_e^2$. ⊙ calculated from $1/R_{centre}$; △ calculated from $(P/P_0)(1/R_{centre})$, Method B; × calculated from r_e^2, Method A. In all three cases the reference time t_1 is 10 sec. The curves are calculated from those representing the observations in Figures 4 and 7.

Information on the radiant power P emitted by a glow cloud can be calculated from the model using equation (6a). When the cloud is non-Gaussian, the radiant power is determined from a numerical integration of the observed radiance distribution. A typical result for P is shown in Figure 9. Overall rate constants can be calculated from the variation of P with time, as indicated in the figure; however, in the case of resonant scattering, allowance must be made for the time dependence of the incident solar flux. Detailed results giving radiant power and centre-point radiance in absolute units will be given in a later paper, together with results obtained using other equipment.

VI. Temperature of Atmosphere

The upper atmospheric properties such as density and temperature are deduced from the observed diffusion coefficient. Chapman and Cowling (1952) derive the relation between these quantities using the kinetic theory of gases; their result for

a rigid, elastic sphere model is

$$D = \frac{3}{8\rho\sigma^2}\left(\frac{kTmM}{\pi}\right)^{\frac{1}{2}}, \tag{8}$$

where

ρ = density, M = molecular weight,
k = Boltzmann's constant, T = temperature,
m = mass of hydrogen atom, σ = molecular collision diameter.

Subsequently, account will be taken of the variation of collision diameter with temperature by using a more realistic molecular model.

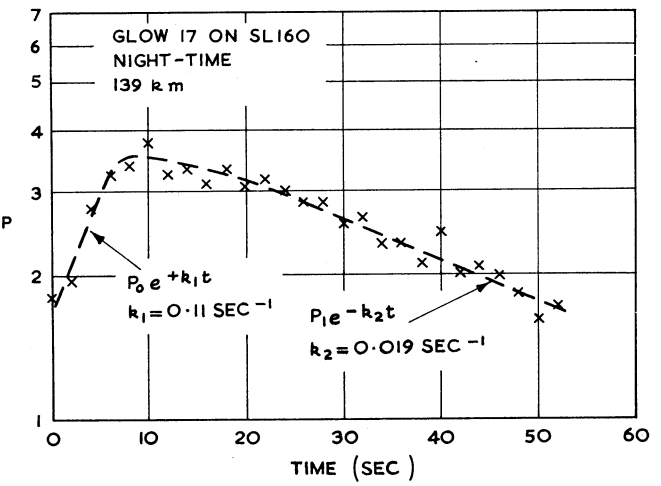

Fig. 9.—Example illustrating variation of radiant power with time.

Equation (8) may be written in terms of the pressure p to give

$$D = \frac{3}{8p\sigma^2}\frac{(kT)^{3/2}}{(\pi mM)^{\frac{1}{2}}}. \tag{9}$$

In order to deduce ρ from D in equation (8), it is necessary to have estimates of M, σ, and T. The model atmospheres of Harris and Priester (1962) are particularly useful because they give results throughout the solar cycle. The parameter S used to describe the solar cycle is based upon the intensity of the 10·7 cm solar flux falling on the Earth, and its value varies from about 250 at sunspot maximum to about 90 at sunspot minimum. Its value in 1963 was about 100 (Harris and Priester 1963).

For the interdiffusion of two gases whose molecular weights are M_1 and M_2, the molecular weight M in equation (8) is given by $2M_1M_2/(M_1+M_2)$. For AlO ($M_2 = 43$) diffusing in air, the fractional increase in $\sqrt{M}$ above the atmospheric value $\sqrt{M_1}$ is 1·16 for $M_1 = 21$ and 1·10 for $M_1 = 28$. At 200 km altitude, the atmospheric molecular weight is unlikely to lie outside the limits 21 and 25; at lower altitudes the difference between the limits is less, so the maximum error in $\sqrt{M}$ will be 3%.

For the calculation of density, the values of M_1 given by Harris and Priester (1962) for $S = 100$ are used.

The accuracy of the results for D justifies taking into account the variation in collision diameter with temperature. The results of Hirschfelder, Curtiss, and Bird (1954) for the Lennard-Jones six-twelve potential model are used to do this. This model expresses the collision diameter σ of equation (8) as

$$\sigma^2 = \sigma_0^2 \, \Omega^{(1,1)*}(T^*),$$

where σ_0 is independent of temperature but depends on the molecular species, $\Omega^{(1,1)*}(T^*)$ is a tabulated function of $T^* = T(\epsilon/k)^{-1}$, and ϵ/k depends on the molecular species. Hirschfelder, Curtiss, and Bird quote σ_0 and ϵ/k for many gases. Plotting these as a function of molecular weight shows that both these quantities increase slowly, and more or less linearly, with molecular weight. The average trend can be represented by $\sigma_0 = 3{\cdot}63 \times 10^{-10}$ m, $\epsilon/k = 80°$K at $M = 28$, and $\sigma_0 = 3{\cdot}90 \times 10^{-10}$ m, $\epsilon/k = 150°$K at $M = 43$. For the interdiffusion of two gases, Hirschfelder, Curtiss, and Bird recommend using the mean values $\sigma_0 = \frac{1}{2}(\sigma_1 + \sigma_2)$ and $\epsilon = (\epsilon_1 \epsilon_2)^{\frac{1}{2}}$. This gives values $\sigma_0 = 3{\cdot}77 \times 10^{-10}$ m and $\epsilon/k = 117°$K for the diffusion of AlO in air. Since $\Omega^{(1,1)*}(T^*)$ is a slowly varying function of T^*, the relatively wide range in possible values of ϵ/k is not critical. For instance, values for T^* of 4, 6, and 8 give values for $\Omega^{(1,1)*}$ of 0·8836, 0·8124, and 0·7712 respectively. The probable error in σ is estimated to be about 4%.

Whereas the atmospheric molecular weight at a given altitude in the range 100–200 km can be estimated with an error of at most 6%, temperature estimates may be seriously in error. At 200 km altitude, the atmospheric temperature during 1963 could possibly lie between 550°K and 1000°K. It is necessary, therefore, to make an estimate of temperature from the observations of diffusion coefficient. This is done from the diffusion scale height, which describes the rate of change of diffusion coefficient with altitude h. Since pressure scale height H_p is defined by $H_p^{-1} = -\partial(\ln p)/\partial h$, the scale height H_q of any altitude-dependent quantity q will be defined by $H_q^{-1} = -\partial(\ln q)/\partial h$. Taking the natural logarithm of equation (9) and differentiating with respect to h gives

$$H_D^{-1} = -H_p^{-1} + \tfrac{3}{2}H_T^{-1} - \tfrac{1}{2}H_M^{-1} - 2H_\sigma^{-1}. \tag{10}$$

It should be observed that H_D is negative and that, in the altitude range of interest, H_T also is negative; that is, $|H_D^{-1}| > H_p^{-1}$.

On the assumption that the atmosphere is a perfect gas, $H_p = RT/M_1 g$. Therefore, if H_p is calculated from the observed value of H_D using equation (10), an estimate of the value of T for the atmosphere may be obtained. The calculation of H_p from H_D may be done in one of two ways.

(1) Using tabulated values from a model atmosphere, the expression $\frac{3}{2}H_T^{-1} - \frac{1}{2}H_M^{-1} - 2H_\sigma^{-1}$ is calculated at several altitudes. This is added to the observed value of $-H_D^{-1}$ to give H_p^{-1}.

(2) Using tabulated values from a model atmosphere, the ratio H_p^{-1}/H_D^{-1} is calculated at several altitudes. The observed value of H_D^{-1} is multiplied by this ratio to give H_p^{-1}.

Of these two possibilities, the second method was chosen. An advantage of this second method is that it allows an estimate to be made of temperature gradient $\partial T/\partial h$, using the identity $H_T^{-1} = -(1/T)\ \partial T/\partial h$. By using tabulated values from a model atmosphere, the ratio H_T^{-1}/H_D^{-1} is calculated at several altitudes. The observed value of H_D^{-1} is multiplied by this ratio to give H_T^{-1}, from which a temperature gradient is obtained by multiplying $-H_T^{-1}$ by the temperature determined from the pressure scale height. The errors in the temperature gradient so determined are likely to be very large; this is because H_T^{-1}/H_D^{-1} changes greatly throughout the solar cycle. Fortunately, this does not matter, because these values of temperature gradient are used solely to smooth the temperature values deduced from pressure scale height.

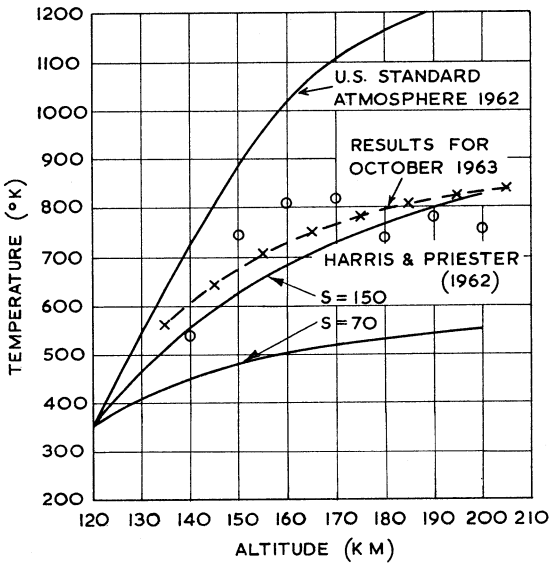

Fig. 10.—Atmospheric temperature. ○ calculated from H_p; $-\times-\times-$ smoothed using $\partial T/\partial h$ (see text).

Figure 10 gives the temperature results for October 1963, derived from the altitude variation of diffusion coefficient using the values of Harris and Priester (1962) for atmospheric molecular weight M_1 and the ratios H_p^{-1}/H_D^{-1} and H_T^{-1}/H_D^{-1} when $S = 100$. The open circles denote the temperatures deduced from H_p, while the crosses show the smoothed values of these temperatures, based on the temperature scale height H_T. The results indicate that the atmospheric temperatures are closer to the temperatures of Harris and Priester (1962) for $S = 150$ than for $S = 100$. If the derivation of temperature from diffusion coefficient is repeated using the values of Harris and Priester (1962) for M_1 etc. at $S = 150$, the results give $T = 540$°K and 930°K at 140 and 200 km altitude respectively. The accuracy of the data, and the uncertainty in the model atmospheric data for M_1, H_p^{-1}/H_D^{-1}, and H_T^{-1}/H_D^{-1}, does not justify a rational choice between these two sets of temperature results. The set for $S = 100$ will be used, with the knowledge that the maximum error is probably about 100°K, i.e. 12%, at 200 km altitude. The earlier (1962) firings shown in

Figure 6 give rather low temperature values; they range from 310°K at 130 km altitude to 470°K at 170 km altitude. Since the errors in diffusion coefficient are much larger for this group of results, the temperatures could be in error by 200°K or so at the higher altitudes.

It should be noted that, since temperature is determined from the rate of change of diffusion coefficient with altitude, several glow clouds should be released from each firing to give an altitude profile of the diffusion coefficient. The accuracy of the density determined from a single release will be poor, unless an estimate of temperature can be made using other data.

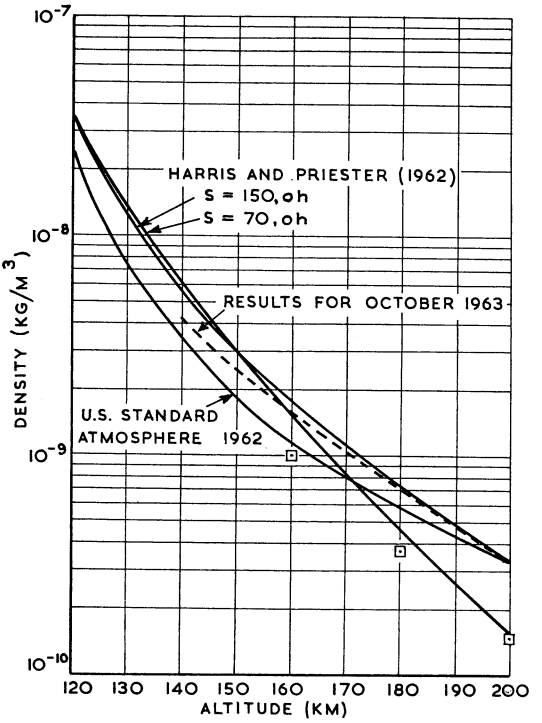

Fig. 11.—Atmospheric density. ⊡ night-time 1963 (King-Hele and Quinn 1965).

Authier, Blamont, and Carpentier (1964) have shown that the temperature at 177 km altitude above Hammaguir was 750°K during evening twilight on February 9, 1964. Figure 10 shows that the temperature at the same altitude above Woomera in October 1963 was 790°K. The good agreement between these two results is significant, since Hammaguir and Woomera both lie in the latitude range 30°–35°. Moreover, Authier, Blamont, and Carpentier relied upon observations of AlO spectra, whereas we have relied upon observations of molecular diffusion coefficient. It seems, therefore, that temperature results obtained from spectral or diffusion observations will be consistent with each other at least over the altitude range 160–200 km.

VII. Density of Atmosphere

We are now in a position to calculate upper atmospheric density from the observed diffusion coefficient, using equation (8). The result for October 1963 using the smoothed temperature results of Figure 10 is shown in Figure 11. If the temperature had been calculated using the $S = 150$ model atmosphere, the derived density would have been 5% less at 140 km and 12% greater at 200 km altitude. As was found for temperature, the observations lie very close to the Harris and Priester (1962) model for $S = 150$, especially above 160 km altitude. Below 160 km altitude, the observed density is less than the Harris and Priester (1962) model but is greater than the U.S. Standard Atmosphere 1962 value. Densities deduced from satellite orbits by King-Hele and Quinn (1965) are given in Figure 11. These densities differ from our results by more than the sum of the errors estimated by us and by King-Hele and Quinn. The reason for such a large difference is not known.

Table 1

RESULTS FROM GLOW CLOUD OBSERVATIONS IN OCTOBER 1963

H_p, T, ρ, n_a, and p have been derived from D as described in Sections VI and VII

h (km)	$D \times 10^{-4}$ (m^2 sec^{-1})	H_p (km)	T (°K)	$\rho \times 10^9$ (kg/m^3)	$n_a \times 10^{-16}$ (m^{-3})	$p \times 10^4$ (N/m^2)
140	0·89	18·0	600	4·24	9·68	8·02
150	1·68	25·6	670	2·41	5·62	5·19
160	2·65	28·4	728	1·61	3·87	3·86
170	4·03	29·6	768	1·09	2·66	2·82
180	6·10	27·6	795	0·729	1·83	2·01
190	8·95	30·1	816	0·502	1·30	1·46
200	13·5	29·9	832	0·334	0·887	1·02

Near 200 km altitude, the density is considerably greater than that deduced from the appropriate model ($S = 100$) of Harris and Priester (1962). The same conclusion is given by Champion (1965), who has reviewed measurements of atmospheric structure in the lower thermosphere and concluded that, in the altitude range 200–230 km, satellite orbit data obtained in 1960 give densities that are greater than those predicted by the models of Harris and Priester (1962). In view of the results given by King-Hele and Quinn, it remains to be seen whether densities deduced from satellite orbits will be in general agreement with those deduced from observations of molecular diffusion coefficient.

Density estimates for 1962 have been obtained by using the temperature results of October 1963 shown in Figure 10, rather than the low temperatures deduced from the diffusion scale height H_D. The densities at 130, 150, and 170 km altitudes were found to be 10×10^{-9}, $3{\cdot}6 \times 10^{-9}$, and $1{\cdot}6 \times 10^{-9}$ kg/m^3 respectively. If the low temperatures indicated by H_D had been used, then the density would decrease from $6{\cdot}8 \times 10^{-9}$ kg/m^3 at 130 km altitude to $1{\cdot}1 \times 10^{-9}$ kg/m^3 at 170 km altitude; these results are very close to those already given for October 1963.

The ambient number density n_a may be calculated from the density by using the relation $n_a = N\rho/M_1$, where N is Avogadro's number. The results for H_p, T, ρ, n_a, and p derived from the October 1963 observations are presented together in Table 1.

The maximum error in the final value of density is about 30%. Contributions to this error arise from diffusion coefficient (15%), temperature (6%), molecular collision diameter (8%), and molecular weight (3%). With improved data-reducing techniques, it should be possible to reduce the errors from the first two sources to 10% and 4% respectively; the error in molecular weight is relatively insignificant. Until a more reliable value for the molecular diameter of AlO can be obtained, the uncertainty in this quantity is irreducible. However, the release of glow clouds with constituents whose molecular collision diameter is known more accurately, such as NO, would reduce the error arising from this source.

VIII. Discussion and Conclusions

Above 160 km altitude, the results for atmospheric density followed the curve for $S = 150$ of the Harris and Priester (1962) model atmosphere. Below 160 km altitude, the observed density was less than the density predicted by this model. The temperatures derived from the results of the second group of firings were also in close agreement with the Harris and Priester (1962) values for $S = 150$. Since the results should have been in agreement with a model atmosphere for $S = 100$, appropriate to October 1963, it seems that the model atmospheres of Harris and Priester (1962) require revision below 200 km altitude. That this should be so is, perhaps, not surprising, since their model atmospheres have been based on satellite density results obtained above 200 km altitude.

The lower limit of the technique of determining density from observed diffusion coefficient is found to be about 130 km altitude. The upper limit for night-time grenade glow clouds appears to be about 155 km altitude; above that altitude, the atmospheric density is so low that the reaction between the glow cloud and the ambient atmosphere results in the formation of only very faint glows. The upper limit for twilight glow clouds is determined by the relative radiance of the glow cloud and of the twilight sky background. The centre-point radiance of twilight glows decreases by about one order of magnitude for an increase in altitude of 50 km. Therefore, provided that the twilight sky background is kept very low, that is, the Earth shadow height is above about 130 km, it should be possible to obtain diffusion coefficients from grenade glow clouds up to about 250 km altitude. Because of absorption of sunlight in the lower layers of the atmosphere, the sunlight is not sufficiently intense to give observable sunlit glows for about 40 km above the Earth's shadow height; that is, when the Earth's shadow is at 130 km, twilight glows can be observed only above 170 km altitude. It follows, unfortunately, that it is not possible to release observable twilight glows throughout the altitude region 130–260 km in one firing. However, since it has been found that twilight and night-time glows give identical values for diffusion coefficient, results over most of this altitude range could be obtained in one firing by observing night-time grenade glow clouds from 130 to 155 km altitude and twilight glow clouds above 170 km altitude.

Because observations can be made only at sunrise and sunset for altitudes above about 155 km, the grenade glow cloud technique cannot be used to determine diurnal changes in density throughout the night. However, it is unlikely that the diurnal effect amounts to more than about 10% at these altitudes, and if there should be a significant effect it would be detected by a morning and an evening twilight firing on the same day.

Temperature and density results for October 1963 have been compared with the only independent results available. The temperature results are in agreement with one measurement obtained from spectral observations of a contaminant release. The density results, on the other hand, differ significantly from those deduced from satellite orbits. The maximum error in density determined by the grenade glow cloud technique is about 30%. This compares very favourably with other methods for determining upper atmospheric density, as reviewed by, for example, Whitehead (1963), who noted that contaminant trail experiments give unsatisfactory measurements of density. Our results show, quite conclusively, that the same criticism cannot be made of the grenade glow cloud technique. However, it must be emphasized that this technique relies upon the generation of optically thin, spherically symmetric glow clouds. Such glow clouds are not necessary if only wind measurements are being made, and either glow cloud or trail techniques can then be used.

The grenade glow cloud technique has the advantage of being direct, and it is not hampered by problems of rocket-borne instrumentation. In particular, interference from rocket outgassing does not exist. The technique gives accurate and reliable data, which are particularly of use in determining the annual changes in density and temperature over the altitude range 130–250 km.

There is still a need for further investigations. Different contaminants should be used so that density and temperature results deduced from aluminized grenade experiments can be compared with other results. The simultaneous use of both pressure gauges and glow clouds to measure atmospheric density is desirable. Scale experiments are also needed to elucidate the mechanisms underlying the generation of large initial cloud radii.

IX. Acknowledgments

The grenade glow cloud experiments were conducted at Woomera as part of the United Kingdom rocket program for upper atmosphere wind measurement. Special observations of the grenade glow clouds were made by the Upper Atmosphere Physics Group, Weapons Research Establishment, and by the Baker–Nunn camera station at Woomera.

The authors wish to thank the Chief Scientist, Australian Defence Scientific Service, Department of Supply, Melbourne, for permission to publish this paper.

X. References

Armstrong, E. B. (1963).—*Planet. Space Sci.* **11**: 743–50.

Authier, B., Blamont, J. E., and Carpentier, G. (1964).—*Annls Géophys.* **20**: 342–5.

Champion, K. S. W. (1965).—*Planet. Space Sci.* **13**: 325–38.

Champion, K. S. W., O'Sullivan, W. J., and Teweles, S. (Eds) (1962).—"U.S. Standard Atmosphere, 1962." (U.S. Government Printing Office.)

CHAPMAN, S., and COWLING, T. G. (1952).—"The Mathematical Theory of Non-uniform Gases." 2nd Ed. pp. 93–9 and 198. (Cambridge Univ. Press.)

CRANK, J. (1956).—"The Mathematics of Diffusion." p. 124. (Oxford Univ. Press.)

GROVES, G. V. (1963*a*).—Intern. Space Sci. Symp. No. 4. pp. 155–70. (Proceedings published as "Space Research. IV".) (North Holland: Amsterdam.)

GROVES, G. V. (1963*b*).—*J. Geophys. Res.* **68**: 3033–47.

HARRIS, I., and PRIESTER, W. (1962).—*J. Geophys. Res.* **67**: 4585–91. Also NASA Tech. Note D-1444 (1962).

HARRIS, I., and PRIESTER, W. (1963).—*J. Geophys. Res.* **68**: 5891–4.

HIRSCHFELDER, J. O., CURTISS, C. F., and BIRD, R. B. (1954).—"Molecular Theory of Gases and Liquids." (Wiley: New York.)

JOHNSON, E. R. (1965).—*J. Geophys. Res.* **70**: 1275–7.

JOHNSON, E. R., and LLOYD, K. H. (1963).—*Aust. J. Phys.* **16**: 490–9.

KING-HELE, D. G., and QUINN, E. (1965).—*Planet. Space Sci.* **13**: 693–705.

LLOYD, K. H. (1965).—*Aust. J. Phys.* **18**: 349–62.

MAY, B. R. (1963).—*Planet. Space Sci.* **11**: 1273–5.

MOLMUD, P. (1960).—*Physics Fluids* **3**: 362–5.

SEDOV, L. I. (1959).—"Similarity and Dimensional Methods in Mechanics." (Translation from 4th Russian edition.) pp. 228, 247. (Infosearch: London; and Academic Press: New York.)

SHEPPARD, L. M., and LLOYD, K. H. (1964).—*Planet. Space Sci.* **12**: 317–18.

WHITEHEAD, J. D. (1963).—*Planet. Space Sci.* **11**: 513–21.